

Propofol attenuates kinesin-mediated axonal vesicle transport and fusion

Madeline Frank, Alec T. Nabb, Susan P. Gilbert¹, and Marvin Bentley^{1,*}

Department of Biological Sciences and Center for Biotechnology and Interdisciplinary Studies, Rensselaer Polytechnic Institute, Troy, NY 12180

ABSTRACT Propofol is a widely used general anesthetic, yet the understanding of its cellular effects is fragmentary. General anesthetics are not as innocuous as once believed and have a wide range of molecular targets that include kinesin motors. Propofol, ketamine, and etomidate reduce the distances that Kinesin-1 KIF5 and Kinesin-2 KIF3 travel along microtubules in vitro. These transport kinesins are highly expressed in the CNS, and their dysfunction leads to a range of human pathologies including neurodevelopmental and neurodegenerative diseases. While in vitro data suggest that general anesthetics may disrupt kinesin transport in neurons, this hypothesis remains untested. Here we find that propofol treatment of hippocampal neurons decreased vesicle transport mediated by Kinesin-1 KIF5 and Kinesin-3 KIF1A ~25–60%. Propofol treatment delayed delivery of the KIF5 cargo NgCAM to the distal axon. Because KIF1A participates in axonal transport of presynaptic vesicles, we tested whether prolonged propofol treatment affects synaptic vesicle fusion mediated by VAMP2. The data show that propofol-induced transport delay causes a significant decrease in vesicle fusion in distal axons. These results are the first to link a propofol-induced delay in neuronal trafficking to a decrease in axonal vesicle fusion, which may alter physiological function during and after anesthesia.

Monitoring Editor

Avital Rodal
Brandeis University

Received: Jul 20, 2022

Revised: Aug 15, 2022

Accepted: Sep 7, 2022

INTRODUCTION

Anesthesia is a key component of modern medical treatment, yet current understanding of anesthetic physiology is fragmentary, at best. General anesthetics, including propofol, impact early brain development and can cause neurodegeneration and long-lasting disruptions in synaptic communication (Lee *et al.*, 2015; Kelz and Mashour, 2019; Maksimovic *et al.*, 2022). Defining the set of molecular targets and mechanism of action of anesthetic drugs is crucial for developing alternative general anesthetics and minimizing side effects.

This article was published online ahead of print in MBoC in Press (<http://www.molbiolcell.org/cgi/doi/10.1091/mbc.E22-07-0276>) on September 14, 2022.

Conflict of interest: The authors declare no competing interest.

Author contributions: M.F. and A.T.N. designed, performed, and analyzed experiments. S.P.G. and M.B. supervised the research, conceptualized the study, designed experiments, and wrote the manuscript.

*Address correspondence to: Marvin Bentley (bentlm3@rpi.edu).

Abbreviations used: DIV, days in vitro; DMSO, dimethyl sulfoxide; KLC, kinesin light chain; NgCAM, neuron-glia cell adhesion molecule; propofol, 2,6-diisopropylphenol; VAMP2, vesicle-associated membrane protein 2 or synaptobrevin-2.

© 2022 Frank *et al.* This article is distributed by The American Society for Cell Biology under license from the author(s). Two months after publication it is available to the public under an Attribution-Noncommercial-Share Alike 4.0 International Creative Commons License (<http://creativecommons.org/licenses/by-nc-sa/4.0>).

"ASCB®," "The American Society for Cell Biology®," and "Molecular Biology of the Cell®" are registered trademarks of The American Society for Cell Biology.

Propofol (2,6-diisopropylphenol) is the most commonly used intravenous general anesthetic (Kotani *et al.*, 2008; Bateman and Kesselheim, 2015; Hemmings *et al.*, 2019) and administered to 30–50 million patients every year (Walsh, 2018). It is thought to act by altering the activity of various ligand- or voltage-gated neuronal channels, including the GABA_A receptor. Propofol is a small, hydrophobic molecule that readily crosses the blood–brain barrier, anesthetizes rapidly, and allows for rapid patient recovery after administration ends. However, despite ~75% of propofol typically clearing within 24 h, adverse side effects caused by propofol include pain on injection, hypotension, hypoventilation, bradycardia, and hyperlipemia (Eckenhoff and Tang, 2018). Propofol has been in clinical use since the 1980s (Walsh, 2018), yet the precise mechanism of action of propofol and the complete set of target proteins remain unknown (Eckenhoff and Tang, 2018).

The motor protein kinesin was recently identified as a novel propofol target (Bensel *et al.*, 2017; Woll *et al.*, 2018). Most kinesins move cargoes by stepping hand-over-hand toward the plus end of microtubules (Asbury *et al.*, 2003; Kaseda *et al.*, 2003; Yildiz *et al.*, 2004). Individual dimers can take more than 1000 consecutive 8 nm steps on a single microtubule, exceeding 10 μm in distance (Soppina *et al.*, 2014). Members of the Kinesin-1, -2, and -3 families are thought to mediate long-range microtubule-based transport in

mammals (Hirokawa *et al.*, 2009, 2010). In single molecule experiments, propofol reduced the run length—the distance moved in a single continuous excursion—of Kinesin-1 (KIF5) and Kinesin-2 (KIF3AB and KIF3AC) motors by 40–60% (Bensel *et al.*, 2017). Further work found that propofol reduces run lengths by binding to the leading head of microtubule-bound kinesins, increasing the probability of dissociation before the lagging head can complete a step (Woll *et al.*, 2018; Dutta *et al.*, 2021). Because the propofol binding pocket forms only when the leading kinesin motor domain is an ATP state and bound to the microtubule, motor dissociation results in propofol release (Woll *et al.*, 2018; Dutta *et al.*, 2021). Consequently, propofol effects are reversible and observable only during acute treatment.

It is unclear whether propofol-mediated attenuation of kinesin stepping affects vesicle transport in cells. Nearly all eukaryotic cells rely on microtubule-based vesicle transport to maintain a functioning endomembrane system (Verhey *et al.*, 2011). Neurons—the target cells of anesthetics—have extreme transport requirements (Bentley and Banker, 2016; Guedes-Dias and Holzbaur, 2019; Nabb *et al.*, 2020; Radler *et al.*, 2020). Human axons can span up to 1 m, and kinesin-mediated vesicle transport supplies the constant need for protein material at the distal axon. In axons, microtubules are densely packed and oriented in parallel, with their plus ends away from the cell body (Baas *et al.*, 1988). This creates an optimal environment for efficient kinesin-mediated anterograde vesicle transport. Vesicles are moved by coordinated groups of kinesins. Consequently, vesicles exhibit run lengths that far exceed those of individual kinesins because multiple kinesins can engage microtubules simultaneously and loss of any one active kinesin can be compensated for by the remaining kinesins. Thus, propofol effects observed in single molecule experiments may not manifest in a physiologically relevant reduction of intracellular vesicle transport.

In this study, we tested the hypothesis that propofol disrupts kinesin-mediated vesicle transport in axons. We found that propofol reduced the run length and velocities of anterograde axonal transport for both Kinesin-1 family member KIF5C and Kinesin-3 family member KIF1A vesicles. This transport delay is associated with the delayed accumulation of neuron–glia cell adhesion molecule (NgCAM), an axonal transmembrane protein that is delivered to the distal axon. Finally, we found that the delay in vesicle transport resulted in decreased fusion of the synaptic membrane protein vesicle-associated membrane protein 2 (VAMP2) in distal axon tips. Taken together, these data point toward a model in which kinesins—possibly all 15 or so kinesins that are thought to mediate vesicle transport—are affected by propofol, resulting in alteration of physiological function during and after anesthesia.

RESULTS

Propofol decreases anterograde Kinesin-1–mediated axonal vesicle transport

To test the hypothesis that propofol affects kinesin-mediated, long-range vesicle transport in cells, we opted for live-cell imaging in cultured hippocampal neurons. Because the propofol effect is best characterized for Kinesin-1 (Bensel *et al.*, 2017; Woll *et al.*, 2018; Dutta *et al.*, 2021), we used a labeling strategy that we recently developed to visualize vesicle-bound Kinesin-1 family member KIF5C (Yang *et al.*, 2019; Frank *et al.*, 2020; Montgomery *et al.*, 2022). We expressed halo-tagged KIF5C tail at low levels in 6–9 days in vitro (DIV) cultured hippocampal neurons and visualized vesicles with JF549 (Grimm *et al.*, 2015). KIF5C binds to vesicles through the kinesin light chain (KLC) (Hackney *et al.*, 1991; Schnapp, 2003; Woźniak and Allan, 2006), and nonfluorescent KLC1a was

coexpressed with KIF5C to maximize vesicle binding. Halo-KIF5C tail can bind and label vesicles, but the absence of a motor domain ensures that all vesicle movements are exclusively mediated by endogenous motors. Vesicles labeled by Halo-KIF5C tail move in axon and dendrites (Yang *et al.*, 2019). Dendrites have a mixed microtubule orientation, half of microtubules with their plus end toward and half away from the distal dendrite. This mixed microtubule organization makes it challenging to determine whether any individual vesicle is moved by plus end–directed kinesins or minus end–directed dynein. In contrast, all axonal microtubules are oriented with their plus end away from the cell body (Baas *et al.*, 1989). Thus, anterograde movement is mediated by kinesin and retrograde movement by dynein (Bentley and Banker, 2016; Guedes-Dias and Holzbaur, 2019). We therefore focused our initial analysis on axonal movement of Kinesin-1 vesicles.

Expressed Halo-KIF5C tail localized to vesicles in the axon and dendrites (Figure 1), in agreement with previous studies (Yang *et al.*, 2019; Frank *et al.*, 2020; Montgomery *et al.*, 2022). High-magnification images show that axonal Halo-KIF5C vesicles were dim, likely due to the relatively small number of kinesins on each vesicle (Figure 1, A and B). The kymographs show that most axonal transport was anterograde. On kymographs, anterograde transport events are indicated by lines with positive slopes and retrograde transport events by lines with negative slopes.

To manage the complexity of imaging vesicle transport in live cells, we designed experiments to isolate propofol effects from those caused by repeated imaging while still measuring the impact of acute propofol treatment on individual cells. Each neuron was recorded twice. An initial recording (“0 min”) was generated before treatment to determine the baseline transport parameters for each cell. Neurons were then treated with dimethyl sulfoxide (DMSO) (vehicle) or 10 μ M propofol for 10 min; a concentration of 10 μ M is within the physiologically relevant range and on the lower end of published concentrations for *in vitro* experiments (Eckenhoff and Tang, 2018; Li *et al.*, 2018). In addition, the studies that first detected a propofol effect on kinesins *in vitro* used the same concentration (Bensel *et al.*, 2017; Woll *et al.*, 2018). After this treatment, cells were recorded a second time (“10 min”). Repeated imaging can result in phototoxicity, which harms cell health and may reduce transport activity independent of propofol. The vehicle control condition (DMSO) accounts for any decrease in trafficking caused by the handling and imaging of the samples, independent of propofol. This experimental design gives confidence that any effect observed in the propofol condition, but not DMSO, is caused specifically by the anesthetic.

Cultured neurons vary in the number of labeled vesicles and their transport parameters. This can be due to the expression level of exogenous constructs or natural cell-to-cell variation in vesicle dynamics. A key strength of this experimental design is that each cell was recorded twice and acts as its own control, minimizing confounding effects caused by cell-to-cell variability. To quantify changes in transport, all analysis was performed by blinded kymograph review. For initial analysis, transport events from all cells in each condition were pooled into a data set and are visualized as histograms (Figure 1, C and D).

Histograms show that the overall anterograde run length at 10 min increased minimally in vehicle control cells (Figure 1C). This change was not statistically different from that at the 0 min time point and highlights the inherent variability in neuronal vesicle transport. Anterograde velocity did not change significantly in the DMSO treatment. In contrast, propofol-treated neurons had ~60% shorter anterograde run lengths after 10 min treatment, with the mean run

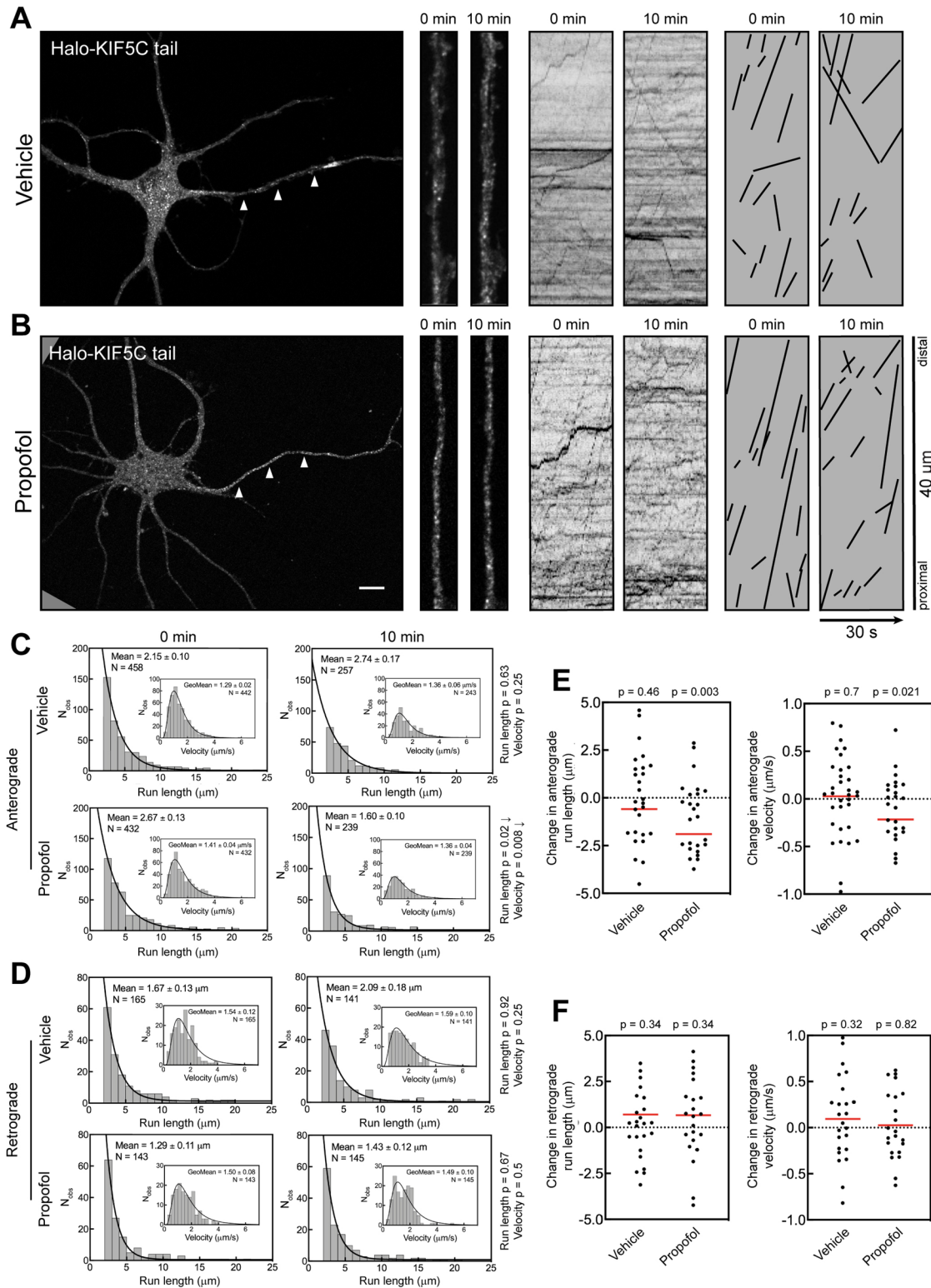


FIGURE 1: Propofol attenuates anterograde transport of axonal KIF5C vesicles. (A, B) Representative images of 7 DIV hippocampal neurons expressing Halo-KIF5C tail and visualized with JF549. Arrowheads indicate the axon. High-magnification images and kymographs show vesicles and axonal transport of Halo-KIF5C vesicles before and 10 min after treatment with (A) vehicle (DMSO) or (B) 10 μ M propofol. For clarity, transport events from kymographs are redrawn as black lines. Kymograph lines with a positive slope indicate anterograde transport, and lines with a negative slope indicate retrograde transport. This convention is followed in all figures. Scale bar: 10 μ m. (C, D) Histograms of axonal run lengths and velocities for axonal vesicles visualized with Halo-KIF5C tail. (E, F) Plots of the change in run length and velocity for each neuron after 10 min treatment with vehicle (DMSO) or propofol. DMSO: 27 cells; propofol: 25 cells.

length decreasing from 2.67 to 1.60 μm . Anterograde velocity also decreased, from 1.41 to 1.36 $\mu\text{m/s}$, which is modest but statistically significant. Notably, the overall number of observed vesicles decreased comparably in both DMSO and propofol conditions as indicated by *N* values in each histogram. The decrease in vesicles is likely due to photobleaching, as KIF5 vesicles are notoriously dim (Yang *et al.*, 2019; Montgomery *et al.*, 2022), which makes them particularly susceptible to photobleaching.

Retrograde axonal transport is mediated by cytoplasmic dynein and not kinesins (Maday *et al.*, 2014; Bentley and Banker, 2016; Guedes-Dias and Holzbaaur, 2019), and the kinesin and dynein microtubule binding domains differ structurally. This makes it unlikely that propofol impacts dynein-mediated transport, although it has not yet been tested experimentally. We analyzed retrograde transport to determine whether propofol effects were specific for kinesin-mediated transport and not due to an overall decline in neuronal health, microtubule stability, or other indirect effects. Neither retrograde run length nor velocity was affected by propofol treatment (Figure 1D). This confirms that the experimental design did not affect overall cell health. Furthermore, these data are strong evidence that propofol does not affect dynein trafficking, a previously unaddressed question.

One potential weakness with this analysis is that particularly active cells, with high numbers of moving vesicles, contribute disproportionately to the data set. To account for such variation, we performed a second analysis in which the change in run length and velocity was quantified for each cell by comparing the 0 and 10 min time points (Figure 1, E and F). The change in run length for each cell was calculated by subtracting the average run length for events at 0 min from the average run length of all the runs at 10 min. The same metric was applied to quantify the change in velocity. In this analysis, each cell contributes one data point, which reduces the overall impact that a single cell with high transport activity can have on the data.

Analysis of the change in transport parameters for individual neurons (Figure 1E) gave results comparable to those based on the histogram data (Figure 1C). Neurons treated with DMSO exhibited no change in anterograde run length and velocity (Figure 1E). Yet, anterograde run length decreased substantially in propofol-treated neurons. This change in run length was accompanied by a decrease in anterograde velocity after propofol treatment ($p = 0.021$). Retrograde run length and velocity were not affected by propofol (Figure 1F), again indicating that propofol does not alter dynein-mediated transport.

These results show that the previously defined effect of propofol on single kinesin motors causes measurable effects on Kinesin-1-mediated axonal vesicle transport in hippocampal neurons. The propofol-induced decrease in vesicle run length is consistent with results from single molecule experiments (Bensel *et al.*, 2017; Woll *et al.*, 2018).

Propofol decreases anterograde axonal transport of Kinesin-3 vesicles

While Kinesin-1s are essential axonal anterograde transporters, the Kinesin-3 family also plays critical roles in neuronal vesicle transport (Silverman *et al.*, 2010; Bentley and Banker, 2016; Guedes-Dias and Holzbaaur, 2019; Nabb *et al.*, 2020; Cason and Holzbaaur, 2022). It is not known whether Kinesin-3 family members are affected by propofol, as *in vitro* analysis of these motors has not yet been performed.

To determine whether the propofol effect observed with vesicles moved by Kinesin-1 (Figure 1) also applied to Kinesin-3 vesicles, we

expressed KIF1A-GFP to visualize vesicles and applied the same experimental strategy as before. Expression of full-length KIF1A results in relatively consistent vesicle labeling, which is unusual among kinesins and differs starkly from that of KIF5 (Yang *et al.*, 2019; Montgomery *et al.*, 2022). KIF1A is a Kinesin-3 family member that mediates anterograde axonal transport of a variety of cargoes, including brain-derived neurotrophic factor (Lo *et al.*, 2011) and presynaptic vesicles (Niwa *et al.*, 2008). KIF1A vesicles underwent robust axonal transport (Figure 2, A and B), consistent with previous studies (Niwa *et al.*, 2008; Decker *et al.*, 2010; Lo *et al.*, 2011; Yang *et al.*, 2019; Frank *et al.*, 2020). First, we quantified the run length and velocity for KIF1A vesicles (Figure 2C). There was no significant change in the run length of KIF1A-labeled vesicles after DMSO treatment. In contrast, propofol treatment resulted in an ~25% decrease in mean run length, dropping from 3.47 to 2.60 μm . The retrograde run length remained unchanged in both treatments, confirming that propofol did not indiscriminately affect vesicle transport or neuron health. The anterograde velocity of KIF1A-GFP movement decreased from 2.54 to 2.07 $\mu\text{m/s}$ in propofol-treated axons. This outcome contrasted with DMSO-treated neurons in which velocity increased from 2.39 to 2.54 $\mu\text{m/s}$. It is unlikely that light exposure during imaging increased the velocity of KIF1A vesicles. Instead, there may be more variability in KIF1A-mediated transport, potentially because KIF1A mediates the transport of a large range of neuronal vesicles that likely have differences in their transport parameters (Niwa *et al.*, 2008; Lo *et al.*, 2011; Jenkins *et al.*, 2012; Hung and Coleman, 2016; Tanaka *et al.*, 2016; Stucchi *et al.*, 2018). Therefore, the observed variability in KIF1A vesicle velocities could be caused by the inherent diversity of KIF1A vesicles. This interpretation is strengthened by the fact that neither retrograde run length nor velocity was changed by DMSO or propofol treatment (Figure 2D).

Analysis of transport changes in individual neurons (Figure 2, E and F) gave results that were comparable to those in the entire vesicle population (Figure 2, C and D). Anterograde run lengths were substantially decreased by propofol, and although anterograde velocity was decreased, this change was not statistically significant in this analysis (Figure 2E). Retrograde run length and velocity were not affected in either condition (Figure 2F).

Propofol attenuates anterograde axonal transport of NgCAM vesicles

During transport, motor ensembles consisting of multiple kinesins participate in the movement of a single vesicle. One potential complication with imaging fluorescent kinesins on vesicles is that individual kinesins can cycle on and off vesicles during imaging. Vesicle detachment of fluorescent kinesins could visually end a run due to the vesicle losing its fluorescent label, with the now invisible vesicle continuing its movement. To address this concern, we analyzed vesicles labeled with a transmembrane cargo molecule that is not directly involved in transport. We chose NgCAM (Jareb and Banker, 1998; Silverman *et al.*, 2001; Petersen *et al.*, 2014; Nabb and Bentley, 2022), a type I transmembrane protein that moves in axonal vesicles transported by Kinesin-1 (Yang *et al.*, 2019). We exposed neurons expressing NgCAM-GFP to the same imaging regiment and DMSO/propofol treatment as in previous experiments (Figure 3). As expected, axonal NgCAM vesicles underwent long-range transport with a strong anterograde bias (Figure 3, A and B). The 10 min DMSO treatment did not affect anterograde run length and velocity (Figure 3C). In contrast, propofol treatment reduced the anterograde NgCAM run length from 3.04 to 2.18 μm , a nearly 30% decrease (Figure 3C), less than the decrease in run length observed with Kinesin-1-labeled vesicles but nonetheless substantial

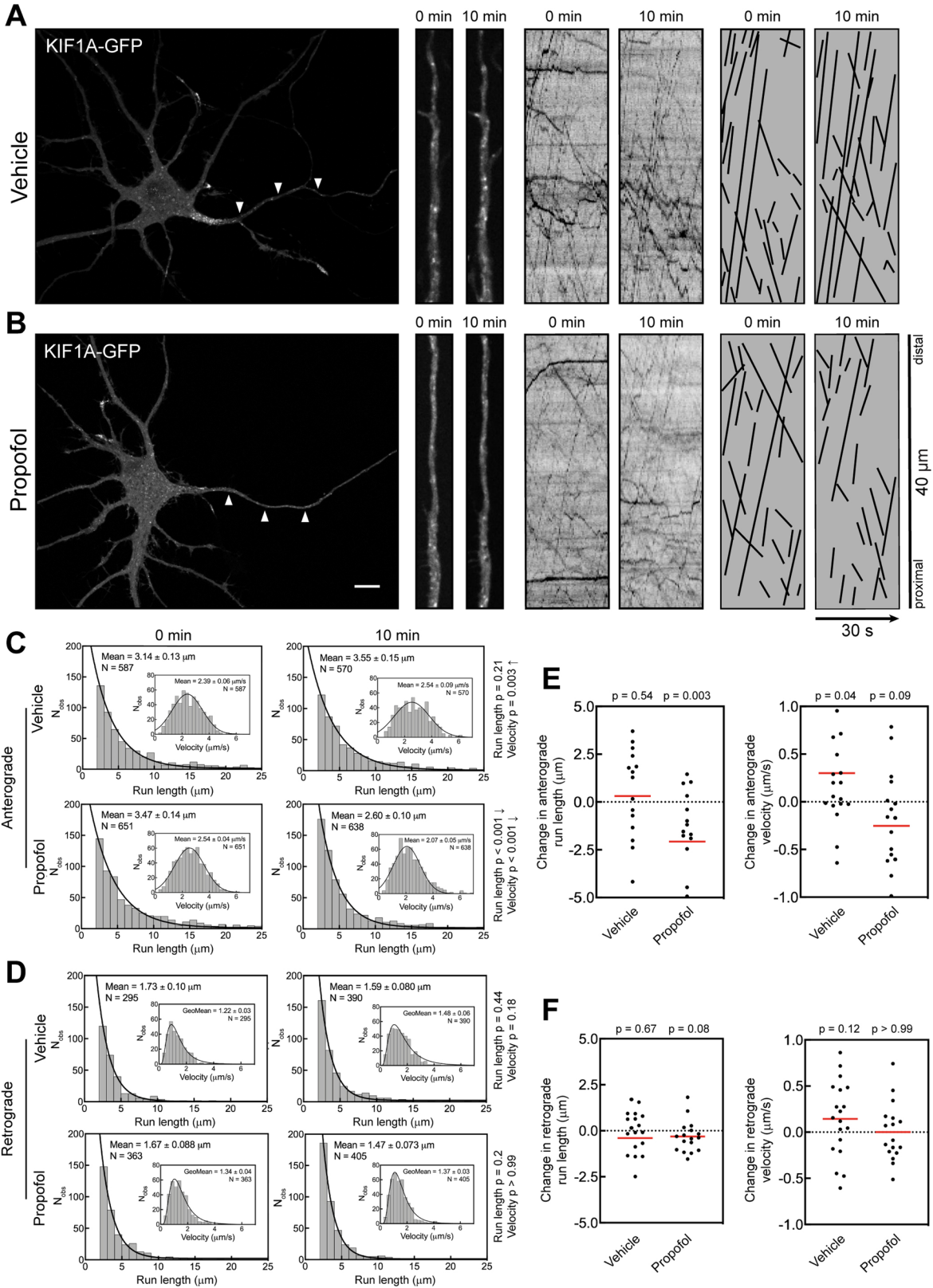


FIGURE 2: Propofol attenuates anterograde transport of axonal KIF1A vesicles. (A, B) Representative images of 7 DIV hippocampal neurons expressing KIF1A-GFP. Arrowheads indicate the axon. High-magnification images and kymographs show vesicles and axonal transport of KIF1A-GFP before and 10 min after treatment with (A) vehicle (DMSO) or (B) 10 μM propofol. For clarity, transport events from kymographs are redrawn as black lines. Scale bar: 10 μm. (C, D) Histograms of axonal run lengths and velocities for axonal vesicles visualized with KIF1A-GFP. (E, F) Plots of the change in run length and velocity for each neuron after 10 min treatment with vehicle (DMSO) or propofol. DMSO: 15 cells; propofol: 14 cells.

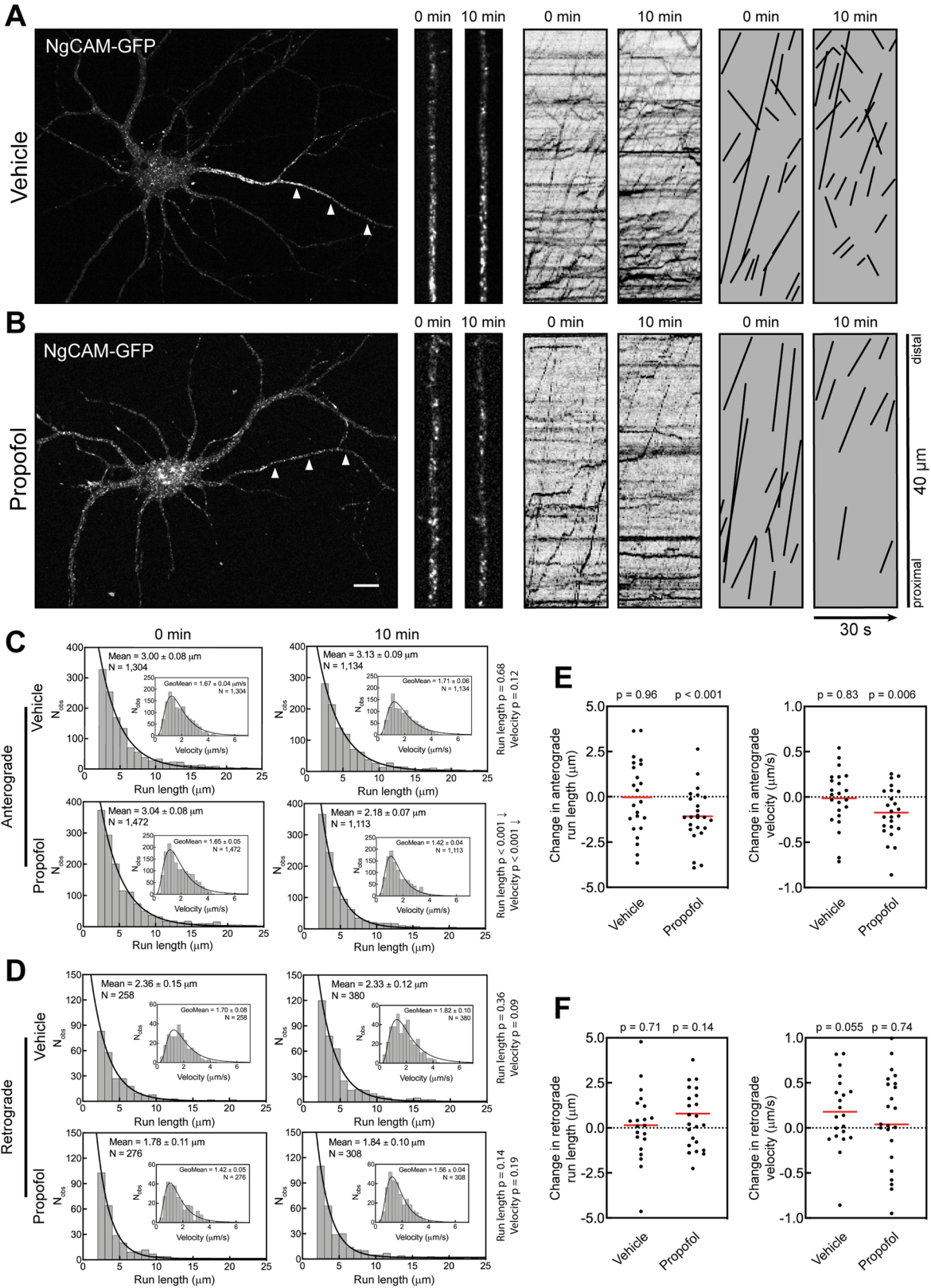


FIGURE 3: Propofol attenuates axonal transport of the KIF5C cargo NgCAM. (A, B) Representative images of 7–8 DIV hippocampal neurons expressing NgCAM-GFP. Arrowheads indicate the axon. High-magnification images and kymographs show vesicles and axonal transport of NgCAM-GFP vesicles before and 10 min after treatment with (A) vehicle (DMSO) or (B) 10 μ M propofol. For clarity, transport events from kymographs are redrawn as black lines. Scale bar: 10 μ m. (C, D) Histograms of axonal run lengths and velocities for axonal vesicles visualized with NgCAM-GFP. (E, F) Plots of the change in run length and velocity for each neuron from 0 to 10 min treatment with vehicle (DMSO) or propofol. DMSO: 21 cells; propofol: 23 cells.

(Figure 1). Propofol treatment also modestly reduced the anterograde velocity of NgCAM vesicles from 1.65 to 1.42 $\mu\text{m/s}$. Analysis of transport changes in each cell also showed a decrease in anterograde run length (Figure 3D), yet that decrease was not statistically significant.

Analysis of retrograde NgCAM transport in the axon found that neither run length nor velocity was affected by propofol (Figure 3, D and F). This again confirmed that the propofol effects are specific for kinesin-mediated anterograde transport.

These results show that propofol treatment decreases axonal transport of kinesin-mediated vesicle movement. The question remains whether the short-term effect of decreasing vesicle run lengths is sufficient to affect the delivery of cargo to the distal axon.

Propofol attenuates protein delivery to the distal axon

We next asked whether the attenuation of vesicle transport caused by propofol results in decreased cargo delivery to the distal axon. To test this hypothesis, we developed an assay to measure the delivery of newly synthesized NgCAM to the distal axon. For detection of newly delivered protein we used the halotag system (Los *et al.*, 2008; Encell, 2012). The halotag enzyme is not independently fluorescent. Instead, fluorescence is conferred only after covalent binding to a ligand with an organic dye. Because the enzyme–substrate reaction results in a covalent bond, interaction with a ligand prevents the halotag enzyme from binding additional ligands. This property, combined with sequential exposure to the spectrally distinct ligands JF646 and JF549 (Grimm *et al.*, 2015), can specifically visualize newly synthesized proteins (Yoon *et al.*, 2016).

We expressed NgCAM-Halo for 12 h and treated cells with JF646 to saturate the halotag binding sites of expressed NgCAM-Halo. This treatment defines a starting point ($t = 0$ h; Figure 4A) for the experiment. Only NgCAM-Halo synthesized after JF646 wash-out can interact during the subsequent JF549 substrate exposure. Therefore, any JF549-labeled NgCAM-Halo at axon tips must have undergone vesicle transport from the soma to the distal axon after the original JF646 saturating treatment.

After JF646 saturation, neurons were incubated with vehicle (DMSO) or propofol for an extended time course (Figure 4, B and C). At each time point, neurons were treated with JF549 and fixed. Images of JF549 (Figure 4B) and JF646 (Figure 4C) were acquired from the soma and the distal axon. In the somata, JF549 staining was concentrated at the Golgi and there was no significant difference in Golgi intensity between DMSO- and propofol-treated neurons at any point in the time course, indicating that propofol did not affect expression levels (Figure 4D).

The upper limit of NgCAM delivery to the distal axon was determined by omitting the JF646 treatment and labeling only with JF549 at the starting time point, 12 h after transfection (0 h; Figure 4A). In all other conditions, JF646 treatment saturation defined the start of the experiment. Axonal delivery of NgCAM was determined by measuring the JF549 intensity in axon tips (Figure 4E). We also determined the axon-to-Golgi-intensity ratio (Figure 4, F and G) for each condition, to account for potential cell-to-cell variation in expression level by using the Golgi intensity as a proxy for expression. DMSO- and propofol-treated neurons both reached comparable axon labeling at 12 h. Four hours after release, the axon-to-Golgi ratio indicated that NgCAM-Halo delivery to the distal axon had plateaued in DMSO-treated cells and remained consistent for the remainder of the time course (Figure 4, F and G). Propofol-treated neurons exhibited a substantial delay in NgCAM-Halo appearance at the distal axon. The lag behind DMSO-treated cells was most significant at the 4 h time point. At 8 h after saturation, propofol-

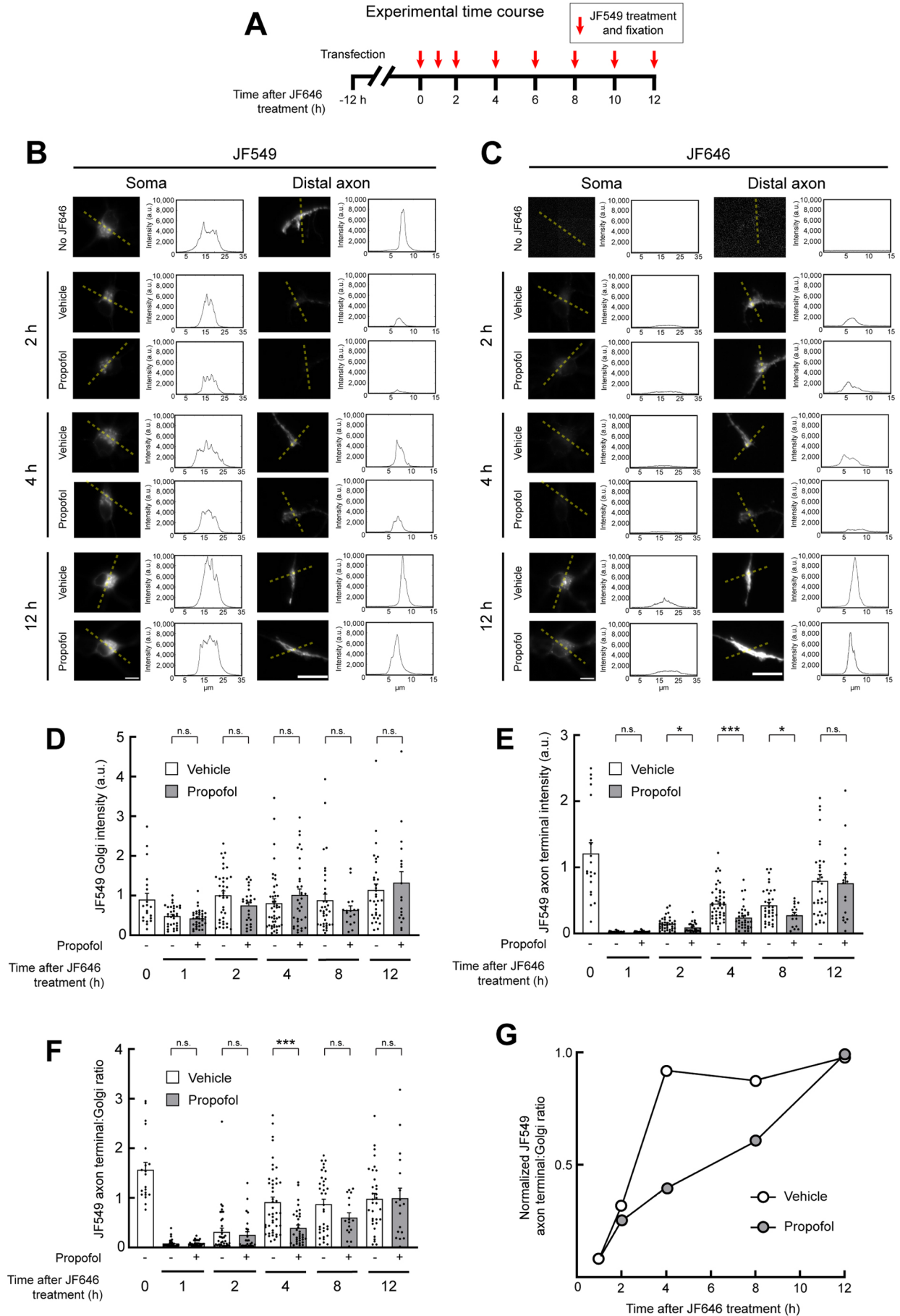
treated axons still had not reached the maximum intensity. Steady-state maximum axonal labeling was reached in both conditions at 12 h. These results show that the propofol effects on kinesins that attenuate vesicle transport are sufficient to cause a delay in cargo delivery to the distal axon.

Propofol-induced transport delay decreases vesicle fusion in distal axons

The decrease in transport and cargo delivery caused by propofol may impact vesicle fusion at axon tips. KIF1A participates in axonal transport of presynaptic vesicles (Okada *et al.*, 1995; Niwa *et al.*, 2008), which can be visualized by expression of GFP-tagged, vesicle-associated membrane protein-2 (VAMP2 or synaptobrevin-2) (Sampo *et al.*, 2003; Lewis *et al.*, 2011; Nabb and Bentley, 2022). Because both anterograde axonal transport of KIF1A vesicles and NgCAM delivery—a cargo that cotransports with VAMP2 (Nabb and Bentley, 2022)—were impacted by propofol, we hypothesized that prolonged treatment with propofol would result in decreased fusion of VAMP2 in distal axon tips. VAMP2 mediates both spontaneous and Ca^{2+} -triggered synchronized fusion of synaptic vesicles (Schoch *et al.*, 2001; Deák *et al.*, 2004; Südhof and Rothman, 2009). Vesicles maintain a stable pool of synaptic vesicles that can act as a “buffer” to maintain spontaneous vesicle release even if vesicle resupply is inhibited for short periods (Fernandez-Alfonso and Ryan, 2008; Fredj and Burrone, 2009). Despite this vesicle buffer, prolonged attenuation of vesicle delivery to axons may result in decreased vesicle fusion. Therefore, decreased VAMP2 fusion due to long-term propofol treatment would be consistent with the model that a propofol-induced decrease in trafficking reduces the number of available fusogenic vesicles in the distal axon.

To visualize spontaneous vesicle fusion, we expressed VAMP2 tagged with the pH-sensitive GFP superrecliptic pHluorin in its C-terminal ectodomain (VAMP2-pHluorin) (Miesenböck *et al.*, 1998; Sankaranarayanan *et al.*, 2000; Barg *et al.*, 2010; Gupton and Gertler, 2010; Kennedy *et al.*, 2010; Keith *et al.*, 2012; Hiester *et al.*, 2017; Bakr *et al.*, 2021). VAMP2-pHluorin is quenched in the acidic lumen of transport vesicles and becomes fluorescent only when the vesicle fuses with the plasma membrane, where pHluorin is exposed to the culture medium at a neutral pH. Vesicle fusion events manifest as bright flashes at the plasma membrane, followed by rapid lateral diffusion and loss of signal (Figure 5). Neurons expressing VAMP2-pHluorin were treated with the vehicle control (DMSO) to determine background levels of vesicle fusion. Propofol affects neuronal channels involved in electrochemical signaling in neurons (e.g., GABA, NMDA, glycine, and serotonin receptors) (Eckenhoff and Tang, 2018; Kelz and Mashour, 2019). To account for nontransport effects, some neurons were exposed to propofol for 1–3 min before recording. This treatment would not impact long-range, microtubule-based transport, but accounts for any immediate propofol effects, for example those on receptors already in the plasma membrane. To identify transport-mediated effects, neurons were treated with propofol for 5 h before imaging. Any newly synthesized VAMP2-pHluorin undergoing kinesin-mediated anterograde axonal transport would be affected by propofol. For each condition, we measured the number of fusion events in the growth cone of distal axons (Figure 5, B and C). The quantifications show that while short-term propofol treatment affected synaptic vesicle release as expected, long-term propofol treatment exacerbated this outcome, consistent with the effect being caused by decreased kinesin-mediated axonal transport.

These data support a model in which the overall fusion capacity at the presynapse is decreased due to a transport defect, causing a



decrease in synaptic vesicle fusion. Because propofol has many target proteins, and because of the complexity that underlies axonal vesicle fusion, other contributing factors cannot be ruled out. However, these results are the first evidence to suggest that a propofol-mediated decrease in axonal transport may contribute significantly to decreased synaptic vesicle fusion in live neurons and that propofol could plausibly alter physiological function during and after anesthesia by targeting kinesins.

DISCUSSION

The principal goal of this study was to determine whether propofol's effect on kinesins impacts vesicle transport in live axons, an environment optimized for efficient vesicle transport. We found consistent attenuation of anterograde axonal transport mediated by Kinesin-1 and Kinesin-3 family members. Moreover, this effect on vesicle trafficking causes defects in cargo delivery to, and vesicle fusion at, the distal axon. These data are the first evidence that propofol alters neuronal vesicle transport and suggest that this interaction is an important physiological effect for anesthesia.

The complement of vesicle-associated kinesins only marginally exceeds resistant forces during vesicle transport

At first glance, it may seem counterintuitive that a modest reduction in the run length of individual kinesins can substantially impact intracellular vesicle transport. Even in the presence of propofol, kinesin dissociation from a microtubule is a relatively rare event. Propofol effects on kinesins were characterized previously by measuring the translocation of single kinesin dimers where exposure to 10 μ M propofol reduced the mean run length of a dimer ~40%, from 1.0 to 0.58 μ m (Bensel *et al.*, 2017), distances that correlate with 125 and 72 processive 8 nm steps, respectively. In contrast, vesicle transport is thought to be mediated by multiple kinesins that are thought to provide redundancy in case any individual kinesin fails. However, such kinesin redundancy has not been tested experimentally. Moreover, the number of kinesins that bind a vesicle during transport and actively translocate along a microtubule is not clear, as such measurements in cells are technically challenging.

The observation that propofol inhibits vesicle transport may give some insight into the composition of kinesin ensembles participating in vesicle transport. To move a vesicle, a kinesin ensemble must overcome forces that resist anterograde movement, that is, drag. This drag is the combination of various factors that include the viscosity of the cytoplasm, interactions of membrane proteins with other cellular components, resistant motor proteins such as dynein and myosin, and other factors. If the combined number of active kinesins produced forces far exceeding the resisting drag force on the vesicle, a modest decrease in each kinesin's processivity would not impact vesicle transport. In this scenario, the loss of one or two kinesins would be compensated for by the remaining active motors.

However, our data are consistent with a model in which the number of engaged kinesins exceeds drag forces by only a relatively small margin as evidenced by two key findings. First, minimizing the

force surplus may maximize the energy efficiency of transport by not having unneeded kinesins actively engaged in transport, but also makes transport vulnerable to even modest disruptions. In this scenario, detachment of a small number of active kinesins—perhaps as few as two or three—would rapidly redistribute the load across the remaining kinesins and substantially impact a vesicle's movement, resulting in decreased run lengths. The fact that propofol reduces vesicle run lengths strongly favors this interpretation. Second, a small force surplus model can also account for one key difference between *in vitro* analysis (Bensel *et al.*, 2017) and neuronal vesicle transport: in single molecule experiments, kinesin velocity was not affected by propofol, whereas our experiments found a modest, yet consistent, decrease in vesicle velocity in propofol-treated cells. As the load on individual kinesins increases, there is a corresponding decrease in velocity (Svoboda and Block, 1994; Schnitzer *et al.*, 2000). We therefore speculate that the premature loss of even a few active kinesins on the vesicle would cause a considerable load increase on the remaining kinesins, resulting in both a decrease in vesicle velocity and a reduction in overall run length.

Taken together, these data argue that vesicle transport is energy efficient, with little margin in active motors beyond what is necessary to overcome resisting forces. Propofol may become a useful tool in future experiments to determine the force surplus for moving vesicles and how many kinesins are involved in each vesicle's movement.

Propofol as an inhibitor of anterograde axonal transport

On the basis of our results, we speculate that propofol may broadly impact anterograde axonal transport. In this study, propofol affected the transport of vesicles moved by members of the Kinesin-1 and Kinesin-3 families. Previous work found that heterotrimeric KIF3AB and KIF3AC, members of the Kinesin-2 family, were affected similar to Kinesin-1, exhibiting substantially decreased run length in the presence of propofol (Bensel *et al.*, 2017). The Kinesin-1, -2, and -3 families are thought to mediate most anterograde axonal vesicle transport (Hirokawa *et al.*, 2009; Verhey *et al.*, 2011; Bentley and Banker, 2016; Nabb *et al.*, 2020), and together these families consist of 15 transport kinesins. Because representative members of these families have been found susceptible to propofol effects, propofol may impact most, if not all, anterograde axonal transport. While this study is focused on axons, neuronal dendrites can grow to up to 1 mm in length and also require kinesin-mediated vesicle transport for maintenance (Bentley and Banker, 2016; Radler *et al.*, 2020). Future studies will determine whether postsynaptic maintenance and function are impacted by trafficking defects caused by propofol treatment.

The mechanism by which propofol binds Kinesin-1 was recently defined (Woll *et al.*, 2018; Dutta *et al.*, 2021). Propofol binds at the kinesin neck linker when the leading head is bound to the microtubule in an ATP state (Woll *et al.*, 2018). The kinesin motor domains that propofol binds are highly evolutionarily conserved (Miki *et al.*, 2005; Wickstead and Gull, 2006; Wickstead *et al.*, 2010). This suggests the possibility that all members of the

FIGURE 4: Propofol delays delivery of membrane proteins to the distal axon. (A) Schematic showing the experimental design. Twelve hours after transfection with NgCAM-Halo, neurons were incubated in JF646 dye to saturate existing NgCAM-Halo binding sites. After JF646 washout, NgCAM-Halo was treated with JF549 and fixed at the indicated time points. (B, C) Representative images of NgCAM-Halo labeled by JF549 (B) or JF646 (C) in the soma and distal axon of neurons, visualized and fixed at the indicated time points after JF646 saturation. Dotted lines indicate the areas from which intensity plot profiles were generated. Scale bars: 10 μ m. (D, E) Quantification of JF549-labeled NgCAM-Halo at the Golgi (D) and the distal axon (E). (F) Quantification of the axon-to-Golgi JF549 ratio. (G) Golgi-to-axon ratio values plotted as a fraction of the maximal 12 h time point. *P* values: * < 0.05; *** < 0.001.

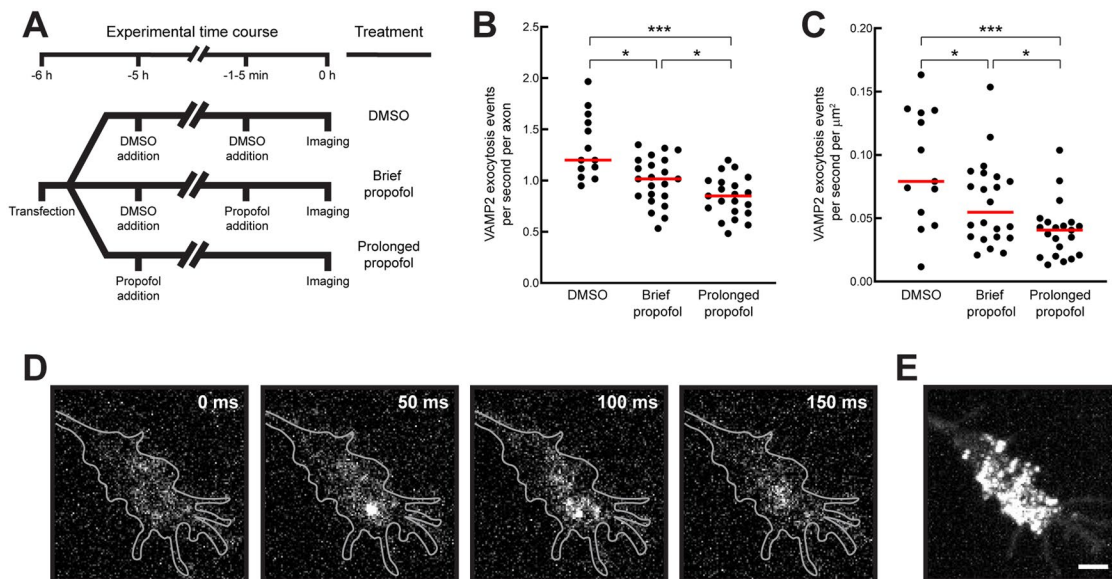


FIGURE 5: Propofol reduces VAMP2 exocytosis in axonal growth cones. (A) Schematic outlining the experimental design. Cells expressing VAMP2-pHluorin were treated with DMSO, 10 μ M propofol for 1–5 min (brief propofol), or 10 μ M propofol for 5 h (prolonged propofol) before imaging. (B, C) Quantification of VAMP2-pHluorin exocytosis events. DMSO: 742 events in 13 growth cones; brief propofol: 703 events in 21 growth cones; prolonged propofol: 624 events in 21 growth cones. (D) Representative images showing a single VAMP2-pHluorin exocytic event in an axonal growth cone. A bright exocytic flash appears in the second frame before diffusing rapidly. (E) Maximum-intensity projection from all frames recorded of the growth cone in D. Many exocytosis events occurred across the growth cone throughout recording. Scale bar: 2 μ m. *P* values: * < 0.05; *** < 0.001.

Kinesin-1, -2, and -3 families are subject to propofol-mediated attenuation. It remains to be determined whether other kinesins, such as those that participate in mitosis or microtubule modification, are similarly affected.

In contrast, we found that dynein-mediated retrograde transport is unaffected by propofol. The microtubule binding sites of dynein and kinesin overlap (Mizuno *et al.*, 2004), but the structure and sequence of kinesin and dynein motor domains are structurally unrelated. This is consistent with the fact that dynein–microtubule interactions do not form a propofol binding site in the same way that kinesin–microtubule interactions do.

Axonal transport defects and impacts on human health

Vesicle transport is crucial for maintaining axons. Ramon y Cajal (1928) recognized that axons that are disconnected from their cell bodies degenerate. Distal axons require constant delivery of protein and lipid material (Futerman and Banker, 1996). In cultured neurons, inhibition of post-Golgi vesicle formation and axonal delivery arrests axonal outgrowth and leads to eventual axonal retraction (Jareb and Banker, 1997). Even minor disruptions to kinesin-mediated axonal transport could lead to neuronal defects. Consequently, a number of kinesin mutations are associated with neuronal diseases (Chevalier-Larsen and Holzbaur, 2006; Lo Giudice *et al.*, 2006; Adalbert and Coleman, 2013; Millecamps and Julien, 2013; Jennings *et al.*, 2017; Dutta *et al.*, 2018; Gabrych *et al.*, 2019; Budaitis *et al.*, 2021).

Propofol has a diverse array of cellular targets, including the GABA_A receptor, voltage-gated ion channels, hyperpolarization-activated cyclic nucleotide-regulated channels, and transient captor voltage channels (Eckenhoff and Tang, 2018; Hemmings *et al.*, 2019). For these, complete propofol metabolism is thought to restore native function. Yet, side effects observed in patients may last beyond complete metabolism of propofol

(Vasileiou *et al.*, 2009; Hernandez *et al.*, 2017; Eckenhoff and Tang, 2018). Effects on kinesins may differ from those on other targets because the capacity of axonal transport is limited. Restoring cargo levels in distal axons after prolonged propofol treatment may take significant time. Such delays could be even more pronounced in elderly patients, because axonal transport declines with age (Milde *et al.*, 2015). The fact that elderly patients are more sensitive to propofol and its associated side effects is consistent with the model that kinesins are an important propofol target (Phillips *et al.*, 2015; Hernandez *et al.*, 2017). Future experiments will determine the contribution of kinesin-related side effects caused by propofol in human patients. In any case, long-term propofol effects on kinesins are likely to profoundly impact neuronal health and development.

MATERIALS AND METHODS

Cell culture

Primary hippocampal neurons were cultured following the Banker method (Kaech and Banker, 2006). E18 rat hippocampi were dissected, trypsinized, dissociated, and plated onto 18 mm glass coverslips coated with poly-L-lysine. Cultured neurons were grown in N2-supplemented MEM and maintained at 37°C with 5% CO₂. Six to 10 DIV neurons were transfected with Lipofectamine 2000 (Thermo Fisher).

Live imaging of axonal transport

Expression times were optimized for maximal labeling with each construct (Table 1; Halo-KIF5C: 4–5 h; KIF1A-GFP: 6–10 h; NgCAM-Halo: 5–9 h).

Recordings were acquired with an Andor Dragonfly built on a Ti2 (Nikon) microscope with a CFI Apo 60 \times 1.49 NA objective (Nikon), two sCMOS cameras (Zyla 4.2, Andor), and total internal reflection fluorescence (TIRF) capability. The imaging stage,

Construct	Construct design	Accession number	Source
Halo-KIF5C tail	Halotag-LYGAGADLGAGAGAGAGAG-ZincFinger-LPGI-KRAB(A)-GGGSGCGSGGGLYKGGGSGGGSGGGP-KIF5C378-955	NM_001107730	Yang et al., 2019
KLC1a	FRB-3myc-LYKGGSGG-KLC1a	NM_001081177.1	Yang et al., 2019
KIF1A-GFP	KIF1A-GGGSGGGSGGPRT-GFP	NM_001294149.1	Frank et al., 2020
NgCAM-GFP	NgCAM-KLGAPRPT-GFP	Z75013	Nabb and Bentley, 2022
NgCAM-Halo	NgCAM-KLGAPRPTMASLEPTTEDLYFQSDND-Halotag	Z75013	Frank et al., 2020
VAMP2-pHluorin	VAMP2-GDPPVAT-pHluorin	M24105	Adapted from Barg et al., 2010

TABLE 1: Expression constructs.

microscope objectives, and cell sample were kept at 37°C in a warmed enclosure (full lexan incubation ensemble; OkoLab). Z-axis movement was controlled with Perfect Focus (Nikon). Live movies were recorded for 30 s at two frames per second. Cells were maintained in Hibernate E medium without phenol red (BrainBits) supplemented with B27 (ThermoFisher; Cat #A3582801) during imaging.

Axons were identified with anti-neurofascin antibody (NeuroMab; Cat #75-027) conjugated to CF405 (Mix-n-Stain CF405S Antibody Labeling Kit; Biotum; Cat #92231) in the imaging medium. Cells expressing constructs with halotag were treated with 50 nM JF549 (Gross et al., 2013) for 10 min and washed with conditioned medium for 10 min before live imaging. After imaging transfected cells for the 0 min time point, 1 µl of DMSO (control) or 1 µl of 10 mM propofol in DMSO was added to the imaging chamber on the microscope for a final propofol concentration of 10 µM. After a 10 min incubation period, the cells were reimaged for the 10 min time point. All cells were imaged with minimal light and exposure to reduce fluorescence bleaching.

Transport analysis

Kymographs were generated with MetaMorph software (Molecular Devices). All analysis was performed by a single blinded analyst. Transport events were traced on the kymographs, and the coordinates were exported to Microsoft Excel for analysis. Each continuous line with a constant slope was scored as a single transport event, and its velocity, run length, and other parameters were calculated. A single vesicle could undergo multiple transport events if there was a distinct pause between each event.

For the run length and velocity histograms, all observations were combined into a single data set. Run length histograms were generated with 1 µm bins and fitted with an exponential decay curve to determine mean run length:

$$y = y_0 + A \left(\frac{-x}{T} \right)$$

where A is the maximum amplitude and T is the mean run length reported as \pm SEM. No observations with run lengths < 2 µm were included in the analysis and are plotted on the graph because short events may not be microtubule-based transport. The number of run lengths < 2 µm was calculated by the exponential decay fit. Because most events were ≤ 25 µm, those > 25 µm were omitted from the histogram but included in calculating the fitted exponential. Velocity histograms were generated with 0.25 µm bins. The NgCAM and KIF5C data were fitted with a lognormal curve, but the KIF1A velocities fit into a Gaussian distribution. Between 17 and 33 cells were evaluated for each condition, including cells from at least two independent cultures.

Cargo accumulation assay

Seven DIV neurons expressed NgCAM-Halo for 12 h and treated with 500 nM JF646 (Gross et al., 2013) to bind all of the folded NgCAM-Halo proteins. Cells were washed twice with conditioned N2 medium and incubated with medium containing DMSO or 10 µM propofol. Cover slips were fixed with 4% paraformaldehyde at 1, 2, 4, 8, and 12 h after the JF646 washout. Fifteen minutes before fixation, neurons were treated with 500 nM JF549. Control cells (0 min) were not exposed to JF646 dye but incubated with JF549 at 12 h and fixed. Cover slips were imaged with an Axio Imager Z1 with a plan-apochromat 63× 1.4 NA objective and an Axiocam 506 mono EMCCD camera. Image analysis was performed in ImageJ/Fiji and Excel. A region of interest was drawn around the Golgi and two to three axon terminals for each cell, and the 20% brightest pixels were identified and their mean intensity determined.

Axonal vesicle fusion assay

Eight DIV neurons were transfected with VAMP2-pHluorin and soluble tdTomato switched to medium containing 0.1% DMSO or 10 µM propofol. At 5–6 h after transfection, coverslips were transferred to the microscope. Neurons in the “Brief propofol” condition were treated with 10 µM propofol for ~5 min before recording. Distal axon tips were identified by the tdTomato fill, and TIRF microscopy images of distal axon tips were recorded at 20 fps for 60 s. A single blinded analyst reviewed the entire data set consisting of recordings from all conditions and identified fusion events in axon tips. Fusion events were identified as individual, bright, emergent puncta that dissipated rapidly.

Statistical analyses

The p values reported in and referring to panels C and D of Figures 1–3 were determined by Mann–Whitney (run length) or two-tailed Student’s t tests, equal variance (velocity) comparing 0 to 10 min in the condition for either DMSO or propofol. The p values reported in panels E and F of Figures 1–3 were determined by Wilcoxon matched-pairs signed rank test (run length) or paired t test (velocity) comparing 0 to 10 min in the condition for either DMSO or propofol. The p values in Figure 4 were generated by one-way Brown–Forsythe analysis of variance (ANOVA) and Dunnett’s post-hoc analysis test. The p values for Figure 5 were generated by one-way ANOVA and Tukey’s post-hoc analysis.

ACKNOWLEDGMENTS

We thank Geraldine Quinones for excellent technical assistance in culturing and maintaining hippocampal neurons. We acknowledge the BioResearch facility at Rensselaer for assistance with husbandry and tissue collection. We thank members of the Bentley lab for their

thoughtful comments on the manuscript. Research reported in this publication was supported by National Institute of Mental Health award R01MH066179 to M.B., National Institute of General Medical Sciences award R37GM054141 to S.P.G., and National Institute of Aging Training Program T32AG057464 to A.T.N. The content is solely the responsibility of the authors and does not necessarily represent the official views of the National Institutes of Health.

REFERENCES

- Adalbert R, Coleman MP (2013). Review: axon pathology in age-related neurodegenerative disorders. *Neuropathol Appl Neurobiol* 39, 90–108.
- Asbury CL, Fehr AN, Block SM (2003). Kinesin moves by an asymmetric hand-over-hand mechanism. *Science* 302, 2130–2134.
- Baas PW, Black MM, Banker GA (1989). Changes in microtubule polarity orientation during the development of hippocampal neurons in culture. *J Cell Biol* 109, 3085–3094.
- Baas PW, Deitch JS, Black MM, Banker GA (1988). Polarity orientation of microtubules in hippocampal neurons: uniformity in the axon and non-uniformity in the dendrite. *Proc Natl Acad Sci USA* 85, 8335–8339.
- Bakr M, Jullié D, Krapivkina J, Paget-Blanc V, Bouit L, Petersen JD, Retailliau N, Breillat C, Herzog E, Choquet D, et al. (2021). The vSNAREs VAMP2 and VAMP4 control recycling and intracellular sorting of post-synaptic receptors in neuronal dendrites. *Cell Rep* 36, 109678.
- Barg S, Knowles MK, Chen X, Midorikawa M, Almers W (2010). Syntaxin clusters assemble reversibly at sites of secretory granules in live cells. *Proc Natl Acad Sci USA* 107, 20804–20809.
- Bateman BT, Kesselheim AS (2015). Propofol as a transformative drug in anesthesia: insights from key early investigators. *Drug Discov Today* 20, 1012–1017.
- Bensel BM, Guzik-Lendrum S, Masucci EM, Woll KA, Eckenhoff RG, Gilbert SP (2017). Common general anesthetic propofol impairs kinesin processivity. *Proc Natl Acad Sci USA* 114, E4281–E4287.
- Bentley M, Banker G (2016). The cellular mechanisms that maintain neuronal polarity. *Nat Rev Neurosci* 17, 611–622.
- Budaitis BG, Jariwala S, Rao L, Yue Y, Sept D, Verhey KJ, Gennerich A (2021). Pathogenic mutations in the kinesin-3 motor KIF1A diminish force generation and movement through allosteric mechanisms. *J Cell Biol* 220, e202004227.
- Cason SE, Holzbaur ELF (2022). Selective motor activation in organelle transport along axons. *Nat Rev Mol Cell Biol*, DOI: 10.1038/541580-022-00491.
- Chevalier-Larsen E, Holzbaur ELF (2006). Axonal transport and neurodegenerative disease. *Biochim Biophys Acta* 1762, 1094–1108.
- Deák F, Schoch S, Liu X, Südhof TC, Kavalali ET (2004). Synaptobrevin is essential for fast synaptic-vesicle endocytosis. *Nat Cell Biol* 6, 1102–1108.
- Decker H, Lo KY, Unger SM, Ferreira ST, Silverman MA (2010). Amyloid- β peptide oligomers disrupt axonal transport through an NMDA receptor-dependent mechanism that is mediated by glycogen synthase kinase 3 β in primary cultured hippocampal neurons. *J Neurosci* 30, 9166–9171.
- Dutta M, Diehl MR, Onuchic JN, Jana B (2018). Structural consequences of hereditary spastic paraplegia disease-related mutations in kinesin. *Proc Natl Acad Sci USA* 115, E10822–E10829.
- Dutta M, Gilbert SP, Onuchic JN, Jana B (2021). Mechanistic basis of propofol-induced disruption of kinesin processivity. *Proc Natl Acad Sci USA* 118, e2023659118.
- Eckenhoff R, Tang P (2018). Recent progress on the molecular pharmacology of propofol. *F1000Research* 7, 123.
- Encell LP (2012). Development of a dehalogenase-based protein fusion tag capable of rapid, selective and covalent attachment to customizable ligands. *Curr Chem Genomics* 6, 55–71.
- Fernandez-Alfonso T, Ryan TA (2008). A heterogeneous “resting” pool of synaptic vesicles that is dynamically interchanged across boutons in mammalian CNS synapses. *Brain Cell Biol* 36, 87–100.
- Frank M, Citarella CG, Quinones GB, Bentley M (2020). A novel labeling strategy reveals that myosin Va and myosin Vb bind the same dendritically polarized vesicle population. *Traffic* 21, 689–701.
- Fredj NB, Barrone J (2009). A resting pool of vesicles is responsible for spontaneous vesicle fusion at the synapse. *Nat Neurosci* 12, 751–758.
- Futerman AH, Banker GA (1996). The economics of neurite outgrowth—the addition of new membrane to growing axons. *Trends Neurosci* 19, 144–149.
- Gabrych DR, Lau VZ, Niwa S, Silverman MA (2019). Going too far is the same as falling short: kinesin-3 family members in hereditary spastic paraplegia. *Front Cell Neurosci* 13, 419.
- Grimm JB, English BP, Chen J, Slaughter JP, Zhang Z, Revyakin A, Patel R, Macklin JJ, Normanno D, Singer RH, et al. (2015). A general method to improve fluorophores for live-cell and single-molecule microscopy. *Nat Methods* 12, 244–250.
- Gross GG, Junge JA, Mora RJ, Kwon H-B, Olson CA, Takahashi TT, Liman ER, Ellis-Davies GCR, McGee AW, Sabatini BL, et al. (2013). Recombinant probes for visualizing endogenous synaptic proteins in living neurons. *Neuron* 78, 971–985.
- Guedes-Dias P, Holzbaur ELF (2019). Axonal transport: driving synaptic function. *Science* 366, eaaw9997.
- Gupton SL, Gertler FB (2010). Integrin signaling switches the cytoskeletal and exocytic machinery that drives neuritogenesis. *Dev Cell* 18, 725–736.
- Hackney DD, Levitt JD, Wagner DD (1991). Characterization of $\alpha 2 \beta 2$ and $\alpha 2$ forms of kinesin. *Biochem Biophys Res Commun* 174, 810–815.
- Hemmings HC, Riegelhaupt PM, Kelz MB, Solt K, Eckenhoff RG, Orser BA, Goldstein PA (2019). Towards a comprehensive understanding of anesthetic mechanisms of action: a decade of discovery. *Trends Pharmacol Sci* 40, 464–481.
- Hernandez BA, Lindroth H, Rowley P, Boncyk C, Raz A, Gaskell A, García PS, Sleight J, Sanders RD (2017). Post-anaesthesia care unit delirium: incidence, risk factors and associated adverse outcomes. *Br J Anaesth* 119, 288–290.
- Hiester BG, Bourke AM, Sinnen BL, Cook SG, Gibson ES, Smith KR, Kennedy MJ (2017). L-type voltage-gated Ca²⁺ channels regulate synaptic-activity-triggered recycling endosome fusion in neuronal dendrites. *Cell Rep* 21, 2134–2146.
- Hirokawa N, Niwa S, Tanaka Y (2010). Molecular motors in neurons: transport mechanisms and roles in brain function, development, and disease. *Neuron* 68, 610–638.
- Hirokawa N, Noda Y, Tanaka Y, Niwa S (2009). Kinesin superfamily motor proteins and intracellular transport. *Nat Rev Mol Cell Biol* 10, 682–696.
- Hung COY, Coleman MP (2016). KIF1A mediates axonal transport of BACE1 and identification of independently moving cargoes in living SCG neurons. *Traffic* 17, 1155–1167.
- Jareb M, Banker G (1997). Inhibition of axonal growth by brefeldin A in hippocampal neurons in culture. *J Neurosci* 17, 8955–8963.
- Jareb M, Banker G (1998). The polarized sorting of membrane proteins expressed in cultured hippocampal neurons using viral vectors. *Neuron* 20, 855–867.
- Jenkins B, Decker H, Bentley M, Luisi J, Banker G (2012). A novel split kinesin assay identifies motor proteins that interact with distinct vesicle populations. *J Cell Biol* 198, 749–761.
- Jennings S, Chenevert M, Liu L, Mottamal M, Wojcik EJ, Huckaba TM (2017). Characterization of kinesin switch 1 mutations that cause hereditary spastic paraplegia. *PLoS One* 12, e0180353.
- Kaech S, Banker G (2006). Culturing hippocampal neurons. *Nat Protoc* 1, 2406–2415.
- Kaseda K, Higuchi H, Hirose K (2003). Alternate fast and slow stepping of a heterodimeric kinesin molecule. *Nat Cell Biol* 5, 1079–1082.
- Keith DJ, Sanderson JL, Gibson ES, Woolfrey KM, Robertson HR, Olszewski K, Kang R, El-Husseini A, Dell’Acqua ML (2012). Palmitoylation of A-Kinase anchoring protein 79/150 regulates dendritic endosomal targeting and synaptic plasticity mechanisms. *J Neurosci* 32, 7119–7136.
- Kelz MB, Mashour GA (2019). The biology of general anesthesia from paramecium to primate. *Curr Biol* 29, R1199–R1210.
- Kennedy MJ, Davison IG, Robinson CG, Ehlers MD (2010). Syntaxin-4 defines a domain for activity-dependent exocytosis in dendritic spines. *Cell* 141, 524–535.
- Kotani Y, Shimazawa M, Yoshimura S, Iwama T, Hara H (2008). The experimental and clinical pharmacology of propofol, an anesthetic agent with neuroprotective properties. *CNS Neurosci Ther* 14, 95–106.
- Lee JH, Zhang J, Wei L, Yu SP (2015). Neurodevelopmental implications of the general anesthesia in neonate and infants. *Exp Neurol* 272, 50–60.
- Lewis TL, Mao T, Arnold DB (2011). A role for myosin VI in the localization of axonal proteins. *PLoS Biol* 9, e1001021.
- Li R, Liu H, Dilger JP, Lin J (2018). Effect of propofol on breast cancer cell, the immune system, and patient outcome. *BMC Anesthesiol* 18, 77.
- Lo KY, Kuzmin A, Unger SM, Petersen JD, Silverman MA (2011). KIF1A is the primary anterograde motor protein required for the axonal transport of dense-core vesicles in cultured hippocampal neurons. *Neurosci Lett* 491, 168–173.
- Lo Giudice M, Neri M, Falco M, Sturnio M, Calzolari E, Di Benedetto D, Fichera M (2006). A missense mutation in the coiled-coil domain of the KIF5A gene and late-onset hereditary spastic paraplegia. *Arch Neurol* 63, 284–287.

- Los GV, Encell LP, McDougall MG, Hartzell DD, Karassina N, Zimprich C, Wood MG, Learish R, Friedman Ohana R, Urh M, et al. (2008). HaloTag: a novel protein labeling technology for cell imaging and protein analysis. *ACS Chem Biol* 3, 373–382.
- Maday S, Twelvetrees AE, Moughamian AJ, Holzbaur ELF (2014). Axonal transport: cargo-specific mechanisms of motility and regulation. *Neuron* 84, 292–309.
- Maksimovic S, Useinovic N, Quillinan N, Covey DF, Todorovic SM, Jevtovic-Todorovic V (2022). General anesthesia and the young brain: the importance of novel strategies with alternate mechanisms of action. *Int J Mol Sci* 23, 1889.
- Miesenböck G, De Angelis DA, Rothman JE (1998). Visualizing secretion and synaptic transmission with pH-sensitive green fluorescent proteins. *Nature* 394, 192–195.
- Miki H, Okada Y, Hirokawa N (2005). Analysis of the kinesin superfamily: insights into structure and function. *Trends Cell Biol* 15, 467–476.
- Milde S, Adalbert R, Elaman MH, Coleman MP (2015). Axonal transport declines with age in two distinct phases separated by a period of relative stability. *Neurobiol Aging* 36, 971–981.
- Millecamps S, Julien JP (2013). Axonal transport deficits and neurodegenerative diseases. *Nat Rev Neurosci* 14, 161–176.
- Mizuno N, Toba S, Edamatsu M, Watai-Nishii J, Hirokawa N, Toyoshima YY, Kikkawa M (2004). Dynein and kinesin share an overlapping microtubule-binding site. *EMBO J* 23, 2459–2467.
- Montgomery A, Garbouchian A, Bentley M (2022). Visualizing vesicle-bound kinesins in cultured hippocampal neurons. *Methods Mol Biol* 2431, 239–247.
- Nabb AT, Bentley M (2022). NgCAM and VAMP2 reveal that direct delivery and dendritic degradation maintain axonal polarity. *Mol Biol Cell* 33, ar3.
- Nabb AT, Frank M, Bentley M (2020). Smart motors and cargo steering drive kinesin-mediated selective transport. *Mol Cell Neurosci* 103, 103464.
- Niwa S, Tanaka Y, Hirokawa N (2008). KIF1B β - and KIF1A-mediated axonal transport of presynaptic regulator Rab3 occurs in a GTP-dependent manner through DENN/MADD. *Nat Cell Biol* 10, 1269–1279.
- Okada Y, Yamazaki H, Sekine-Aizawa Y, Hirokawa N (1995). The neuron-specific kinesin superfamily protein KIF1A is a unique monomeric motor for anterograde axonal transport of synaptic vesicle precursors. *Cell* 81, 769–780.
- Petersen JD, Kaech S, Banker G (2014). Selective microtubule-based transport of dendritic membrane proteins arises in concert with axon specification. *J Neurosci* 34, 4135–4147.
- Phillips AT, Deiner S, Mo Lin H, Andreopoulos E, Silverstein J, Levin MA (2015). Propofol use in the elderly population: prevalence of overdose and association with 30-day mortality. *Clin Ther* 37, 2676–2685.
- Radler MR, Suber A, Spiliotis ET (2020). Spatial control of membrane traffic in neuronal dendrites. *Mol Cell Neurosci* 105, 103492.
- Ramon y Cajal S (1928). *Degeneration and Regeneration of the Nervous System* (RM May, Trans.), Oxford, UK: Oxford University Press.
- Sampo B, Kaech S, Kunz S, Banker G (2003). Two distinct mechanisms target membrane proteins to the axonal surface. *Neuron* 37, 611–624.
- Sankaranarayanan S, De Angelis D, Rothman JE, Ryan TA (2000). The use of pHluorins for optical measurements of presynaptic activity. *Biophys J* 79, 2199–2208.
- Schnapp BJ (2003). Trafficking of signaling modules by kinesin motors. *J Cell Sci* 116, 2125–2135.
- Schnitzer MJ, Visscher K, Block SM (2000). Force production by single kinesin motors. *Nat Cell Biol* 2, 718–723.
- Schoch S, Deák F, Königstorfer A, Mozhayeva M, Sara Y, Südhof TC, Kavalali ET (2001). SNARE function analyzed in synaptobrevin/VAMP knockout mice. *Science* 294, 1117–1122.
- Silverman MA, Kaech S, Jareb M, Burack MA, Vogt L, Sonderegger P, Banker G (2001). Sorting and directed transport of membrane proteins during development of hippocampal neurons in culture. *Proc Natl Acad Sci USA* 98, 7051–7057.
- Silverman MA, Kaech S, Ramser EM, Lu X, Lasarev MR, Nagalla S, Banker G (2010). Expression of kinesin superfamily genes in cultured hippocampal neurons. *Cytoskeleton* 67, 784–795.
- Soppina V, Norris SR, Dizaji AS, Kortus M, Veatch S, Peckham M, Verhey KJ (2014). Dimerization of mammalian kinesin-3 motors results in superprocessive motion. *Proc Natl Acad Sci USA* 111, 5562–5567.
- Stucchi R, Plucińska G, Hummel JJA, Zahavi EE, Guerra San Juan I, Klykov O, Scheltema RA, Altelaar AFM, Hoogenraad CC (2018). Regulation of KIF1A-driven dense core vesicle transport: Ca²⁺/CaM controls DCV binding and liprin- α /TANC2 recruits DCVs to postsynaptic sites. *Cell Rep* 24, 685–700.
- Südhof TC, Rothman JE (2009). Membrane fusion: grappling with SNARE and SM proteins. *Science* 323, 474–477.
- Svoboda K, Block SM (1994). Force and velocity measured for single kinesin molecules. *Cell* 77, 773–784.
- Tanaka Y, Niwa S, Dong M, Farkhondeh A, Wang L, Zhou R, Hirokawa N (2016). The molecular motor KIF1A transports the TrkA neurotrophin receptor and is essential for sensory neuron survival and function. *Neuron* 90, 1215–1229.
- Vasileiou I, Xanthos T, Koudouna E, Perrea D, Klonaris C, Katsargyris A, Papadimitriou L (2009). Propofol: a review of its non-anaesthetic effects. *Eur J Pharmacol* 605, 1–8.
- Verhey KJ, Kaul N, Soppina V (2011). Kinesin assembly and movement in cells. *Annu Rev Biophys* 40, 267–288.
- Walsh CT (2018). Propofol: milk of amnesia. *Cell* 175, 10–13.
- Wickstead B, Gull K (2006). A “holistic” kinesin phylogeny reveals new kinesin families and predicts protein functions. *Mol Biol Cell* 17, 1734–1743.
- Wickstead B, Gull K, Richards TA (2010). Patterns of kinesin evolution reveal a complex ancestral eukaryote with a multifunctional cytoskeleton. *BMC Evol Biol* 10, 110.
- Woll KA, Guzik-Lendrum S, Benseal BM, Bhanu NV, Dailey WP, Garcia BA, Gilbert SP, Eckenhoff RG (2018). An allosteric propofol-binding site in kinesin disrupts kinesin-mediated processive movement on microtubules. *J Biol Chem* 293, 11283–11295.
- Woźniak MJ, Allan VJ (2006). Cargo selection by specific kinesin light chain 1 isoforms. *EMBO J* 25, 5457–5468.
- Yang R, Bostick Z, Garbouchian A, Luisi J, Banker G, Bentley M (2019). A novel strategy to visualize vesicle-bound kinesins reveals the diversity of kinesin-mediated transport. *Traffic* 20, 851–866.
- Yildiz A, Tomishige M, Vale RD, Selvin PR (2004). Kinesin walks hand-over-hand. *Science* 303, 676–678.
- Yoon YJ, Wu B, Buxbaum AR, Das S, Tsai A, English BP, Grimm JB, Lavis LD, Singer RH (2016). Glutamate-induced RNA localization and translation in neurons. *Proc Natl Acad Sci USA* 113, E6877–E6886.